Sensorless Control of Standalone BDFIGs based MRAS Observer Using α β axis CW Flux

Alameen K. Ebraheem

State Key Laboratory of Advanced Electromagnetic Engineering and Technology, School of Electrical and Electronic Engineering, Huazhong University of Science and Technology, Wuhan 430074, China and

Department of Electrical and Electronic Engineering, Faculty of Engineering & Technology, Nile Valley University, Atbara, Sudan

Abstract: ***In this paper, a mechanical rotor speed estimator for sensorless control of standalone brushless doubly-fed induction generators (BDFIGs) is addressed using the αβ axis CW-flux based model reference adaptive system (MRAS) estimator. The estimator is integrated in the control method for controlling the frequency and voltage value during various work scenarios. The efficiency of the suggested estimator and control technique is proved by overall simulation performance as illustrated without employing a sensors of the rotor speed, the sensorless control strategy integrating the suggested speed estimator can successfully keep the frequency and amplitude of power winding of voltage fixed at various rotor speeds, during various cases of machine parameters and load changes.***

Keywords: model reference adaptive system (MRAS), Brushless doubly fed induction generators (BDFIGs), sensorless control, αβ axis CW-flux**.**

1. Introduction

In order to the use of brushes and slip ring, the conventional (DFIG) face several disadvantages, like large dimensions, minimum reliability, and large cost desired for repair. Furthermore, the (BDFIG) has absorbed much concentration because of its high precision design and minimum maintenance cost. The control winding (CW) and the power winding (PW) with various numbers of poles to hold the straight connecting among them are contained in the stator, while the rotor is particularly structured to offer the cross-connection among CW and PW [1]-[6]. The BDFIG keeps whole the merits of the conventional DFIG [5]. The standalone BDFIG has appeared very good cost-effective solution of energy for changing speed fixed frequency-ship shaft-based power generation systems. the power winding side converter (PSC) is used to supply the changing frequency excitation current for CW, and the control winding side converter (CSC) contribute dc link same like the PSC is linked to the PW for adjusting the dc link voltage and obtaining the power flow in both directions as shown in Figure1 [6]. The application of physical speed sensors has a lot of disadvantages with respect to hardness, cost, repair, and cabling. Therefore, the sensorless physical speed control is preferred [7].

Recently, the stand-alone BDFIG control methods have been addressed are mostly with speed sensors [8], [9], which will decrease system reliability, increase the cost. In this paper, the αβ control winding-flux MRAS using voltage-oriented control strategy is employed to obtain the sensorless control of standalone BDFIG systems, which can achieve the direct control for the frequency and amplitude of the PW voltage, without using physical speed sensor.

The suggested strategy consists of two models, the reference and the adaptive model employing the αβ control winding-flux. The paper is regulated in the following way. The PW stationary frame model for BDFIG is represented in Section 2. Section 3 addresses the structure of the proposed MRAS estimator. The suggested sensorless control system using the αβ axis control winding-flux MRAS observer is addressed in Section 4. The simulation performance is presented in Section 5. Finally, section 6 is addressed the conclusion.

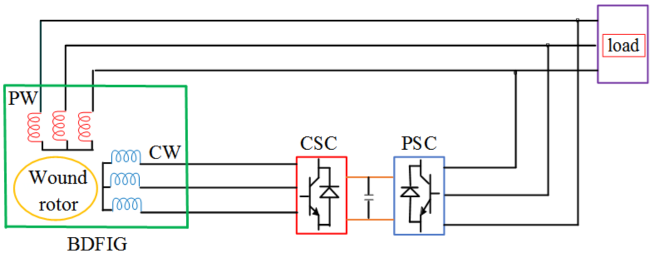

Figure 1: Block diagram of BDFIG

2. Mathematical Model

The mathematical relation for speed of rotor is represented as [10]

$$\omega_r = \frac{\omega_1 + \omega_2}{p_1 + p_2} \quad (1)$$

The equations of BDFIG in the PW stationary frame *(αβ)* is obtained as [10]

$$u_1^{\alpha\beta} = R_1 i_1^{\alpha\beta} + \frac{d\psi_1^{\alpha\beta}}{dt} + j\omega_1\psi_1^{\alpha\beta} \quad (2)$$

$$0 = R_r i_r^{\alpha\beta} + \frac{d\psi_r^{\alpha\beta}}{dt} - jp_1\omega_r\psi_r^{\alpha\beta} \quad (3)$$

$$u_2^{\alpha\beta} = R_2 i_2^{\alpha\beta} + \frac{d\psi_2^{\alpha\beta}}{dt} - j(p_1 + p_2)\omega_r\psi_2^{\alpha\beta} \quad (4)$$

$$\psi_1^{\alpha\beta} = L_1 i_1^{\alpha\beta} + L_1 i_r^{\alpha\beta} \quad (5)$$

$$\psi_r^{\alpha\beta} = L_r i_r^{\alpha\beta} + L_{2r} i_2^{\alpha\beta} + L_{1r} i_1^{\alpha\beta} \quad (6)$$

$$\psi_2^{\alpha\beta} = L_2 i_2^{\alpha\beta} + L_{2r} i_r^{\alpha\beta} \quad (7)$$

where, i, ψ, u, denote current (A), flux linkage (Wb) and voltage (V), respectively, U is RMS value of voltage (V). R_r

R_2 R_1 and L_r L_2 L_1 are resistances (Ω) and Self-inductances (H) of the rotor, control and power windings respectively. While L_{2r}, L_{1r} are mutual inductances (H) among the rotor and control windings; rotor and power windings respectively. Actual rotor positions (mechanical rad) and differential factor is represented by θ_r , and S respectively.

3. MRAS Estimator Structure

The suggested MRAS estimator, as illustrated in Figure 2, has two models, the reference and the adaptive model. The measured flux of CW achieved from the currents and voltages of the PW is compared to the estimated CW-flux achieved from the both currents of the CW and PW. The error is regulated to be converge to zero employing a proportional integral (PI) regulator and the PI regulator output is employed as the observation of the physical rotor speed. Subsequently, this observed speed is fed back to set the adaptive model.

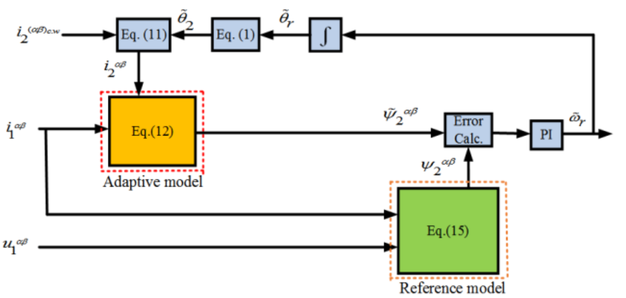

.

Figure 2: Structure of the αβ axis CW-flux MRAS observer

The adaptive model can be obtained as follows.

From (3) and (6), the current of rotor, i_r, can be achieved by

$$i_r^{\alpha\beta} = \frac{\frac{L_{2r}}{L_2}\psi_2^{\alpha\beta} + L_{1r} i_1^{\alpha\beta}}{-\frac{R_r}{(s - jp_1\omega_r)} - L_r + \frac{L_{2r}^2}{L_2}} \quad (8)$$

$R_r/[s - jp_1\omega_r)]$ can be neglected, the rotor current can be obtained as

$$i_r^{\alpha\beta} = \frac{L_{2r}\psi_2^{\alpha\beta} + L_2 L_{1r} i_1^{\alpha\beta}}{L_{2r}^2 - L_2 L_r} \quad (9)$$

From (7), (9), the αβ axis control winding flux is achieved as

$$\psi_2^{\alpha\beta} = \frac{L_2 L_r - L_{2r}^2}{L_r} i_2^{(\alpha\beta_{cw})} - \frac{L_{1r} L_{2r}}{L_r} i_1^{\alpha\beta} \quad (10)$$

The transformation from the CW reference frame ($\alpha\beta_{cw}$), to that in PW reference frame, (αβ) is given as follows

$$i_2^{\alpha\beta} = e^{j(p_1(\hat{\theta}_r+\delta_1)+p_2(\hat{\theta}_r+\delta_2))}(-i_2^{(\alpha\beta_{cw})})^{conj}. \quad (11)$$

Where δ_1, δ_2 denote initial position of PW and CW.

Apply (11) into (10), the adaptive model of the estimation of the αβ axis CW flux can be obtained, as

$$\hat{\psi}_2^{\alpha\beta} = \frac{L_2 L_r - L_{2r}^2}{L_r} i_2^{\alpha\beta} - \frac{L_{1r} L_{2r}}{L_r} i_1^{\alpha\beta} \quad (12)$$

Moreover, a reference model can be designed as follows from (6), and the flux of the rotor is neglected, the following can be achieved

$$0 = L_r i_r^{\alpha\beta} + L_{2r} i_2^{\alpha\beta} + L_{1r} i_1^{\alpha\beta} \quad (13)$$

From (5) and (13), the αβ axis CW current is written as

$$i_2^{\alpha\beta} = -\frac{L_r}{L_{2r} L_{1r}}\psi_1^{\alpha\beta} + \frac{L_r L_1 - L_{1r}^2}{L_{1r} L_{2r}} i_1^{\alpha\beta} \quad (14)$$

From (7), (9) and (14) the reference model of the αβ axis control winding flux is given as

$$\psi_2^{\alpha\beta} = \frac{L_{2r}^2 - L_2 L_r}{L_{1r} L_{2r}}\psi_1^{\alpha\beta} + \frac{L_2 L_1 L_r - L_1 L_{2r}^2 - L_2 L_{1r}^2}{L_{1r} L_{2r}} i_1^{\alpha\beta} \quad (15)$$

The estimated speed of the rotor can be defining as follows

$$\hat{\omega}_r = (K_p + \frac{K_i}{S})(\hat{\psi}_2^{\alpha}\psi_2^{\beta} - \psi_2^{\alpha}\hat{\psi}_2^{\beta}) \quad (16)$$

Figure.3 shows the phase-axis relationships of the PW, CW, and RW of BDFIG

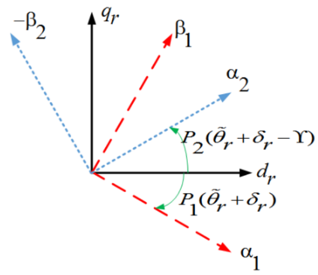

Figure 3: Phase-axis relationships of the PW, CW and RW

4. Suggested Sensorless Control Based on αβ axis control winding-Flux MRAS Observer

The PW voltage d-axis component, u1d tracks the reference of PW voltage U1* through the CW current reference i2d*. The q-axis element PW voltage, u1q, can equal to zero after regulating the CW current frequency, ω2*, such that the overlapping of the resultant PW voltage vector with the d-axis of dq frame, i.e. the PW frequency and voltage can completely track their reference values. (in this paper, the magnitudes of reference are set as 50Hz and 311 V) during various speed of rotor, parameters and load for the standalone BDFIG system. Figure 4 shows the overall proposed control method.

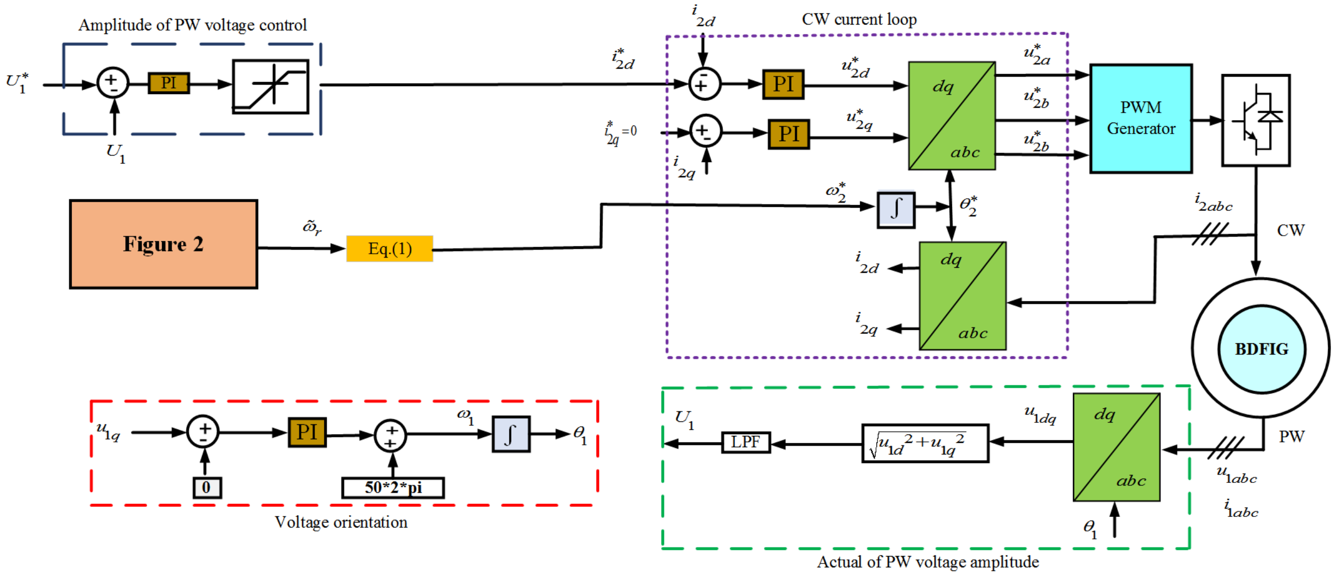

Figure 4: Overall block diagram of the proposed sensorless control method for the standalone BDFIG system

5. Simulation Performance

To prove the implementation of the suggested control technique, several of the achieved results from the simulation are addressed in this part for a BDFIG while the range for variable speed of rotor is, started from 700 rpm and finished with 600 rpm. The effectiveness of the suggested αβ axis control winding-flux MRAS estimator for sensorless DVC during the parameters change is also approved in this part. Table 1 shows the simulated system parameters.

Table 1: Detailed Parameters of BDFIG

Parameter	*Value*
Power	30KVA
Speed domain	600~1200 rpm
p_1, p_2	1,3
The rated of PW current and voltage	380 V, 45 A
The rated of CW voltage	350 V
The rated of CW current	40 A
R_r, R_1, R_2	0.3339 Ω ,0.4034 Ω, 0.2680 Ω
L_r, L_1, L_2	0.2252 H ,0.4749 H, 0.03216 H
L_{1r}, L_{2r}	0.3069 0.02584 H

5.1 Response under Load and Speed Change

Figure 5 shows the response during the speed of the rotor started from 700 rpm and finished with 600 rpm at 1 s for the suggested αβ axis control winding-flux MRAS observer. Figure 6 illustrates the change of load, started from 50 Ω, and finished with 25 Ω at 1 s. Figures. 5(a)-(e) show the measured and observed speeds of rotor, the three phase of PW voltages, the PW dq voltages, the three phase of CW currents, and the three phase of PW currents respectively Figures. 6(a)-(f) show the measured and observed rotor speeds, the three phase of PW voltages, detailed of the three phase of PW voltages, the PW dq voltages, the three phase of CW currents, and the three phase of PW currents respectively.

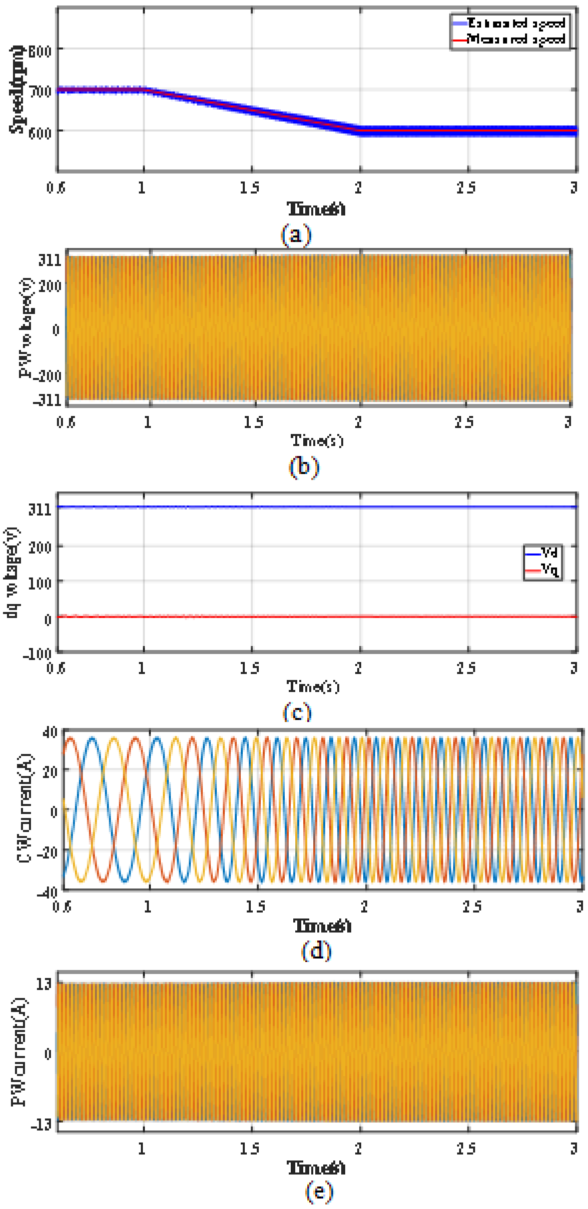

Figure 5: Simulation performances during the speed ramp change. (a) Real and observed speeds of rotor. (b) The three

phase of PW voltages. (c) The PW dq voltages (d) The three phase of CW currents. (e)The three phase of PW currents.

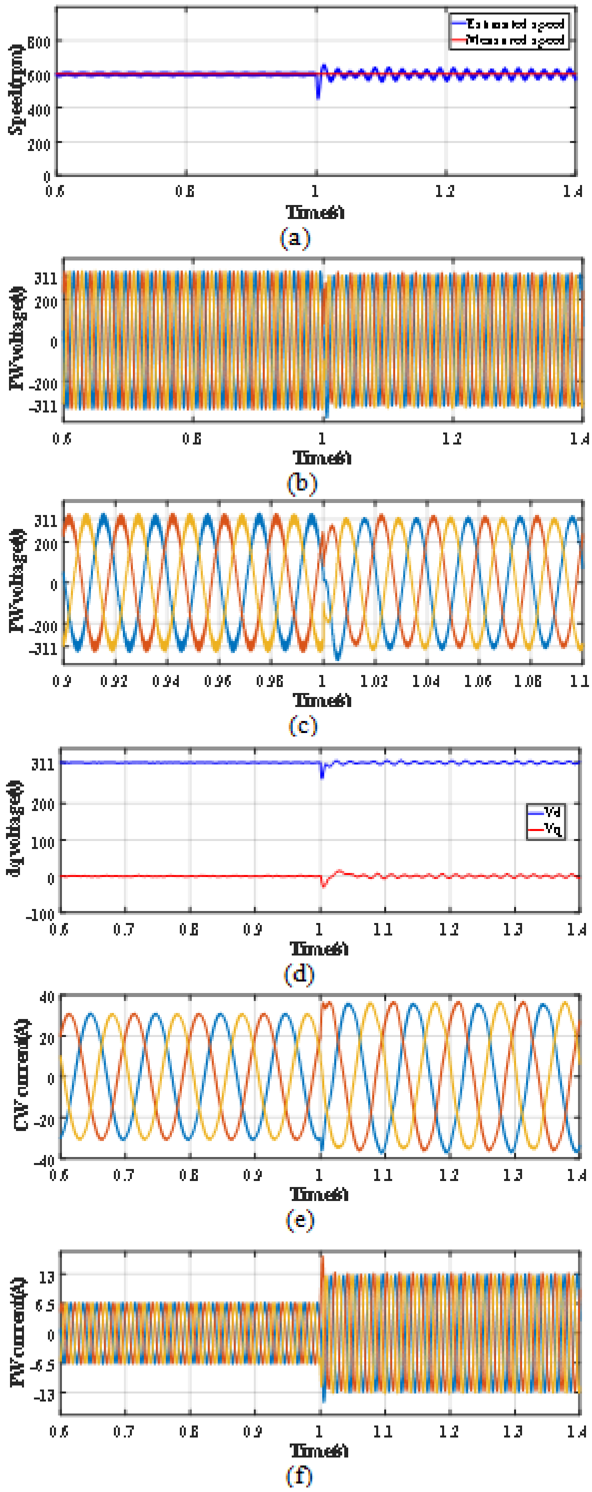

Figure 6: Simulation performances during the load change (a) Real and observed speeds of rotor. (b) The three phase of PW voltages. (c) Detailed of the three phase of PW voltages among 0.9 and 1.1 s(d) The PW dq voltages (e) The three phase of CW currents (f) The three phase of PW currents.

5.2 Effect of Parameters Variations

Figures 7 and 8 illustrate the response of BDFIG when the parameters change, including the change of resistance of PW and whole inductances which affect the proposed control method, respectively. The effects were suggested with 130% of resistance PW and 150% of the all values of inductance under the change of load from 50 Ω to 25 Ω at t=1s. Figures 7 (a)-(f) and 8 (a)-(f) show the measured and observed rotor speeds, the three phase of PW voltages, detailed of the three phase of PW voltages, the PW dq voltages, the three phase of CW currents, and the three phase of PW currents respectively.

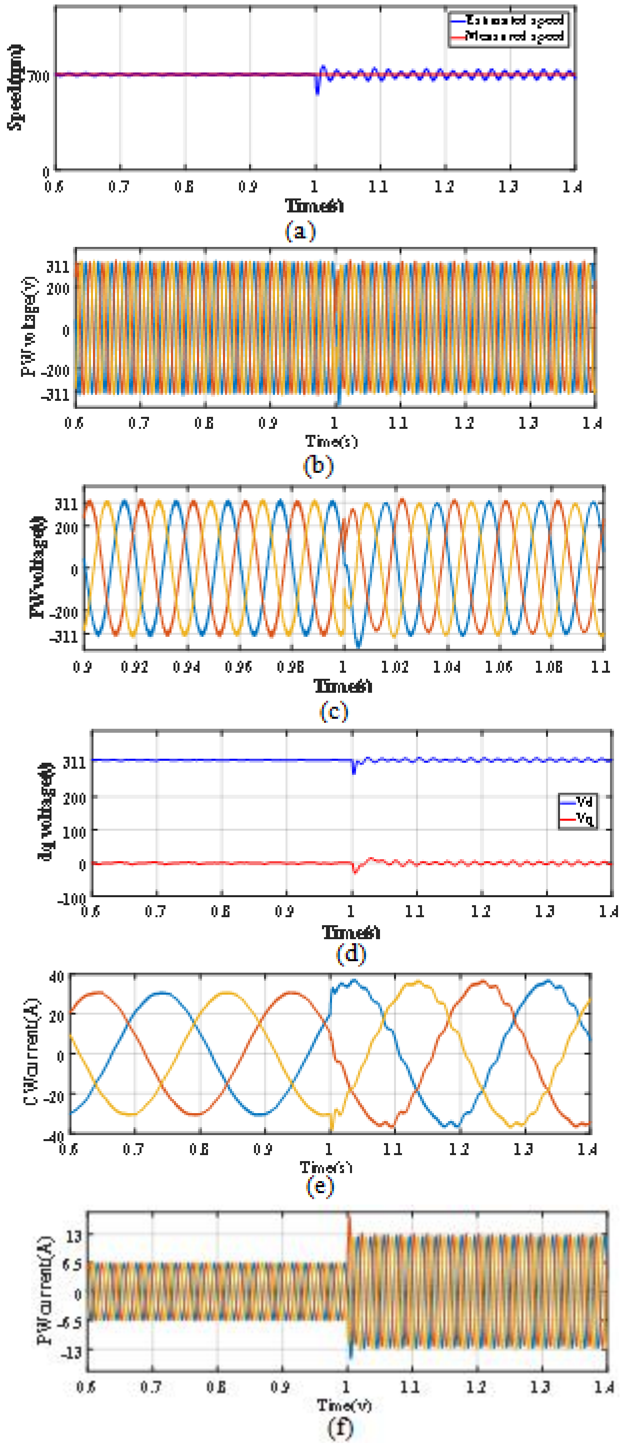

Figure 7: Simulation performances with 130% change in resistance of PW. (a) Real and observed speeds of rotor. (b) The three phase of PW voltages. (c) Detailed of the three phase of PW voltages among 0.9 and 1.1 s(d) The PW dq voltages (e) The three phase of CW currents (f) The three phase of PW currents.

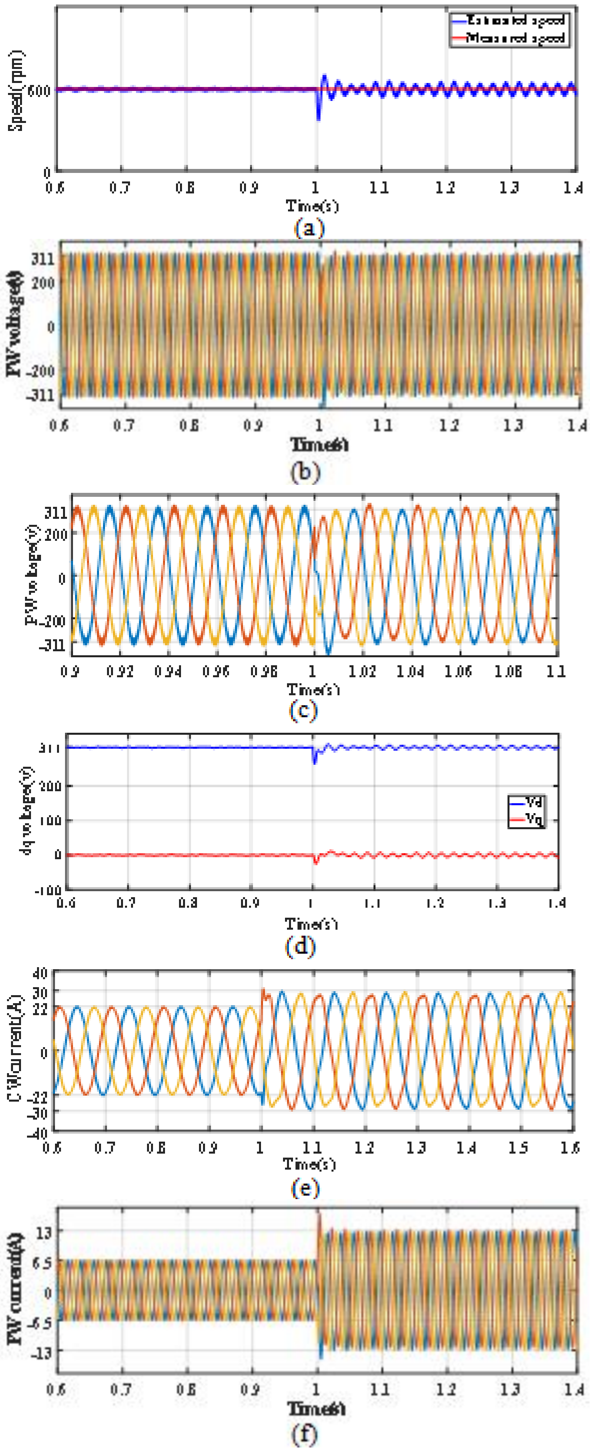

Figure 8: Simulation performances during 150% change in the all inductance. (a) Real and observed speeds of rotor. (b) The three phase of PW voltages. (c) Detailed of the three phase of PW voltages among 0.9 and 1.1 s(d) The PW dq voltages (e) The three phase of CW currents (f) The three phase of PW currents.

6. Conclusion

This paper addresses an MRAS speed observer using αβ axis CW- flux for sensorless control of standalone BDFIG. The validation of the suggested control methodology is shown through simulation performance, the tested BDFIG has proved good transient process during various speeds rotor, parameter changes and load changes through the control of the suggested control strategy using the αβ axis control winding flux MRAS. Furthermore, the performance results prove the good tracking among the observed and real response of speed, proving the robust efficiency of the suggested sensorless control method using the αβ axis control winding flux MRAS observer for standalone BDFIGSs.

References

[1] Teng Long, Shiyi Shao, Ehsan Abdi, Richard A. McMahon, and Shi Liu, "Asymmetrical Low-Voltage Ride Through of Brushless Doubly Fed Induction Generators for the Wind Power Generation," *IEEE Trans. on Energy Convers.*, vol. 28, no. 3, Septemper2013, pp.502-511.

[2] Lei Sun, Yu Chen, Jingyuan Su, Debin Zhang, Li Peng, and Yong Kang, "Decoupling Network Design for Inner Current Loops of Stand-Alone Brushless Doubly Fed Induction Generation Power System," *IEEE Trans. on Power Electron.*, vol. 33, no. 2, February 2018, pp.957-963.

[3] Hamed Gorginpour, Hashem Oraee, and Ehsan Abdi, "Calculation of Core and Stray Load Losses in Brushless Doubly Fed Induction Generators," *IEEE Trans. on Ind. Electron.*, vol. 61, no. 7, July 2014, pp.3167-3177.

[4] Ramtin Sadeghi, Seyed M. Madani, Thomas Anthony Lipo, *Life*, M. R. Agha Kashkooli, Mohammad Ataei, and Sul Ademi, "Voltage-Dip Analysis of Brushless Doubly Fed Induction Generator Using Reduced T-Model," *IEEE Trans. on Ind. Electron.*, vol. 66, no. 10, October 2019, pp.7510-7519.

[5] Ramtin Sadeghi, Seyed M. Madani, M. Ataei, M. R. Agha Kashkooli, and Sul Ademi, "Super-Twisting Sliding Mode Direct Power Control of a Brushless Doubly Fed Induction Generator," *IEEE Trans. on Ind. Electron*, vol. 65, no. 11, November 2018, pp.9147-9156.

[6] Yi Liu, Wei Xu, Teng Long, and Frede Blaabjerg, "An Improved Rotor Speed Observer for Standalone Brushless Doubly-Fed Induction Generator under Unbalanced and Nonlinear loads," *IEEE Power Electron. Regular Paper, in press.*

[7] R. Kumar, S. Das and M. Manohar, "Sensorless control of grid-connected doubly-fed induction machine drive using model reference adaptive controller,"*2016 IEEE Uttar Pradesh Section International Conference on Electrical, Computer and Electronics Engineering (UPCON)*, Varanasi, 2016, pp. 404-409

[8] Y. Liu, W. Ai, B. Chen, K. Chen, "Control design and experimental verification of the brushless doubly-fed machine for stand-alone power generation applications," *IET Elect. Power Appl.*, Vol. 10, No. 1, pp. 25-35, January, 2016.

[9] Y. Liu, W. Ai, B. Chen, K. Chen, and G. Luo, "Control design of the brushless doubly-fed machine for stand-alone VSCF ship shaft generator systems," *J. Power Electron.*, vol. 16, no. 1, pp. 259-267, Jan., 2016.

[10] J. Poza, E. Oyarbide, D. Roye and M. Rodriguez, "Unified reference frame dq model of the brushless

doubly fed machine," *IEE Proc. Electr. Power Appl.*, vol. 153, No. 5, September 2006, pp. 726-734.

Author Profile

Alameen K. Ebraheem received the B.Sc. degree in 2008 from Nile Valley University, Atbara, Sudan in electrical and electronic engineering and the M.Sc. degree in 2012 from Sudan University of Science and Technology, Khartoum, Sudan, in electrical engineering. He was appointed a Lecturer in the Department of Electrical and Electronic Engineering, Faculty of Engineering and Technology, Nile Valley University, Atbara, Sudan, in 2012. From Sept. 2016, he has been pursuing the Ph.D. degree at the State Key Laboratory of Advanced Electromagnetic Engineering and Technology, School of Electrical and Electronic Engineering, Huazhong University of Science and Technology, Wuhan, China. His current research interests include sensorless control, control engineering, AC electrical machine control, and electrical drives.